Assessing interactions among multiple physiological systems during walking outside a laboratory: An Android based gait monitor

E.Sejdić[1,*], A. Millecamps[a], J. Teoli[a], M. A. Rothfuss[a], N. G. Franconi[a], S. Perera[b], A. K. Jones[a], J. S. Brach[c], M. H. Mickle[a]

[a] *Department of Electrical and Computer Engineering, Swanson School of Engineering, University of Pittsburgh, Pittsburgh, PA, USA*
[b] *Division of Geriatric Medicine, University of Pittsburgh, Pittsburgh, PA, USA*
[c] *Department of Physical Therapy, University of Pittsburgh, Pittsburgh, PA, USA*

Abstract

Gait function is traditionally assessed using well-lit, unobstructed walkways with minimal distractions. In patients with subclinical physiological abnormalities, these conditions may not provide enough stress on their ability to adapt to walking. The introduction of challenging walking conditions in gait can induce responses in physiological systems in addition to the locomotor system. There is a need for a device that is capable of monitoring multiple physiological systems in various walking conditions. To address this need, an Android-based gait-monitoring device was developed that enabled the recording of a patient's physiological systems during walking. The gait-monitoring device was tested during self-regulated overground walking sessions of fifteen healthy subjects that included 6 females and 9 males aged 18 to 35 years. The gait-monitoring device measures the patient's stride interval, acceleration, electrocardiogram, skin conductance and respiratory rate. The data is stored on an Android phone and is analyzed offline through the extraction of features in the time, frequency and time-frequency domains. The analysis of the data depicted multisystem physiological interactions during overground walking in healthy subjects. These interactions included locomotion-electrodermal, locomotion-respiratory and cardiolocomotion couplings. The current results depicting strong interactions between the locomotion system and the other considered systems (i.e., electrodermal, respiratory and cardivascular systems) warrant further investigation into multisystem interactions during walking, particularly in challenging walking conditions with older adults.

[*]Corresponding author
Email address: esejdic@ieee.org (E.Sejdić)

Keywords: Gait monitoring, gait accelerometry signals, stride intervals, electrocardiogram, skin conductance, respiratory rate.

1. Introduction

Mobility disabilities in older adults is a major factor in the loss of independence and contributes to higher rates of morbidity and mortality [1] and are considered to be a predictor of other disabilities that restrict independent living [2]. Unfortunately, the clinical identification of impaired gait function is not straightforward. The locomotor function and its associated parameters, including gait speed, are traditionally assessed under ideal conditions without distractions in a well-lit, unobstructed walkway. In patients with subclinical physiological abnormalities, these ideal conditions may not provide enough stress on their ability to adapt to walking. A challenging walking environment can provide a more realistic assessment in the early detection of alterations in walking and in the characterization of subclinical physiological abnormalities. Patients walking on challenging environments have previously been used to detect subclinical risk in aging research. Fall risks were predicted more accurately by gait characteristics on irregular and challenging surfaces when compared to smooth and non-challenging surfaces [3]. The fear of falling (FOF) is highly prevalent for all older adults [4], [5], and is known to negatively impact gait parameters (e.g., reduced gait velocity or higher stride-length or stride-time variability) [6]. Fear also induces significant change in physiological signals, heart rate and skin conductance, associated with cardiovascular and autonomic control systems (e.g., [7], [8], [9]). The interaction between cardiovascular systems, autonomic control systems and their impact on gait function have not been sufficiently quantitatively linked due to the lack of computational methods and instrumentation for the reliable assessment of these systems in real-life scenarios.

Prior gait assessment systems have centered on a single transduction method. Analysis of multiple physiological modalities during gait often required interfacing multiple acquisitions systems together [10]. A widely accepted approach for such interfacing is the use of a stationary system that provides gait temporal-spatial parameters. The GaitMat, a typical representative of the stationary system, consists of a long array of pressure sensitive switches that detect foot strikes upon participant ambulation [11]. These systems provide accurate and reliable measures of temporal-spatial gait parameters during free walking but the limited size and the high cost associated with larger

mats are a deterrent in the widespread use. VICON is another type of stationary system that captures three-dimensional data of gait through the use of video motion capture systems. These video capture systems can accurately and precisely capture gait kinematics [12] but the systems are expensive and require multiple cameras arrangements that must be calibrated in the constrained volume [13]. Although it is possible to extend a video capture system to larger volumes, the cost of the system would scale with the increase in volume. Due to the limited number of steps that can be taken on these stationary systems, concerns exist about the limited analysis of these systems due to the small window lengths in detrended fluctuation analysis [14].

In response to these shortcomings, a number of solutions to gait monitoring have been developed in recent years that aim to assess older adults and patients with walking problems. In addition to these rehabilitation devices, the LOCOMAT [15], active ankle foot orthosis [16] and sensor-embedded shoes have been used to assess the human locomotor function. Examples of this include the ACHILLE system [16], GaitShoe [17], the Intelligent-Shoe [18], and a sensor-embedded shoe measuring ground contact [19]. Devices for the assessment of physiological signals have also been developed that include wrist worn heart rate monitors and wrist worn activity monitors [20]. Additional devices include the FRWD [21], a sport computer that measures heart rate, distance, speed, and altitude, or the SenseWear armband from Bodymedia, a measurement device worn near the biceps [22] capable of measuring skin temperature, galvanic skin response, three-axis accelerations, and heat flux from body. Also, devices such as the Delsys Tringo wireless system have been used to assess electromyography and accelerometry signals during walking (e.g., [23]). Clothing-based physiological monitors such as a LifeShirt from Vivometrics [24], the adiStar Fusion products [25], the VTAMN [26], and the Wealthy measurement system [27] have been developed. Similarly, smartphones have become a popular platform for gait monitoring in recent years (e.g., [28], [29]). However, none of the devices have incorporated the interactions between various physiological systems to understand their impact on the locomotor function. Assessing only gait parameters is not sufficient for the early prediction of falls due to a number of factors that cause gait instabilities. By assessing multisystem interactions, we will be able to make early predictions about falls and warn patients about their instability.

There is a need for a screening instrument that can accurately detect impaired locomotor function outside of controlled settings. In this paper, an Android-based system is proposed for the

simultaneous acquisition of temporal gait parameters including force sensitive resistors (FSR) placed on the heel and forefoot, an electrocardiogram (ECG), electrodermal response (EDR), respiration via a strain gauge transducer, and a tri-axial accelerometer placed on the lumbar region of the spine during ambulation. The proposed system was tested using 15 healthy subjects, and data was collected for verification and preliminary analysis. Our goal was to test the reliability of the system, specifically, to understand whether the system was capable of collecting physiological signals reliably. Therefore, from the data collected and extracted to an external workstation, a number of features, previously considered in other publications, were extracted in time, frequency and time-frequency domains to conduct a preliminary analysis of the interaction between multiple physiological systems and locomotor function.

This paper is organized as follows: In the next section, an overview of the data collection system is provided. Section 3 illustrates the data collection procedure with the data analysis steps outlined in Section 4. Our results and discussions are given in Sections 5 and 6, respectively. Finally, conclusions are drawn in Section 7, followed by a list of references.

2. Collection System Overview

The mobile data collection system is comprised of three main components:

- multiple biosignal transducers attached to the participants with signal conditioning circuitry;
- a microcontroller unit (MCU) that digitizes each biosensor; and
- An Android smartphone that receives data from the MCU and stores it for post-processing.

A high-level overview of the system concept is shown in Figure 1. A phablet computer running the Android operating system is used as the hub for receiving the sensor signals and logging the data. The Android device communicates with a MCU via a USB interface. The MCU essentially provides a bridge to collect and multiplex the sensor signals for communication and storage on the Android device. For many of the sensors, custom signal conditioning circuitry was to accept and multiplex the analog signals into the MCU.

In our particular design, we used a Samsung Galaxy Nexus Android phone to function as the data-logging hub. A Microchip PIC24 (PIC24FJ256GB106) functioned as the MCU. An on-board Parallax H48C tri-axial accelerometer was connected to the MCU via a serial peripheral interface

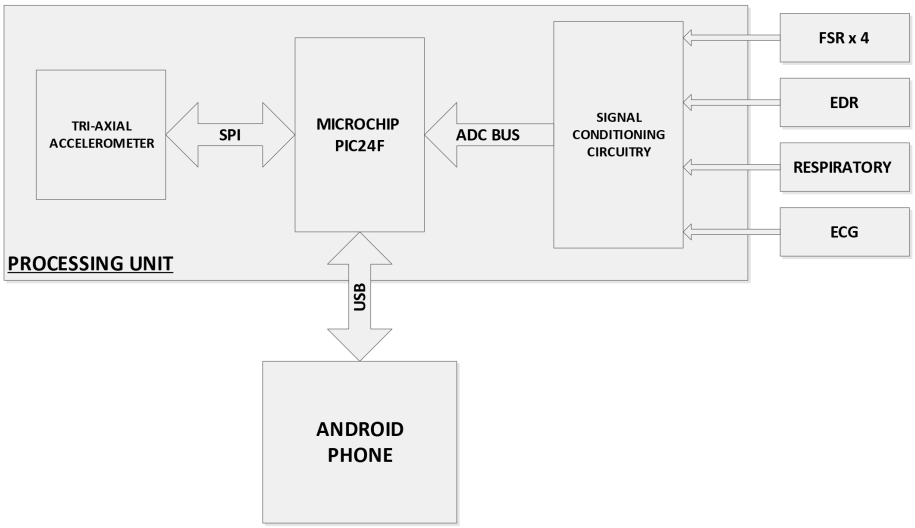

Figure 1: Hardware overview of gait data collection system

(SPI) digital bus. The remaining analog transducers were all discrete components external to the MCU and included electrocardiography electrodes, electrodermal activity electrodes, strain gauges, and force sensitive resistors. The final design was realized using a PCB to integrate the discrete components.

The remainder of this section describes the implementation of the three major components including the design of the signal conditioning circuitry for the analog transducers, the design of the microcontroller code to accept the input sensor signals and relay them to the Android phablet computer, and the data logging software on the Android phablet computer.

2.1. Signal conditioning and transducer details

As described in Figure 1, with the exception of the accelerometer whose output is read digitally, the sensors are designed to deliver analog input to the MCU with an attenuation of at least 30dB at the Nyquist frequency (i.e. half the sample rate). All considered sensors are commercially available sensors, and they are typically used in clinical examinations. In this section we describe the peripheral signal conditioning circuitry to allow the signals to effectively interface with the MCU. The analog transducers and accelerations sampling was performed using time-division multiplexing. We considered first the sampling of analog transducers. As shown on Figure 2, each sensor was sampled successively at a rate of 949 Hz, the sampling duration being 150.5 μs for each of them. Accelerations were sampled at a rate of 1kHz, the sampling duration being 250 μs for each

acceleration as well as a reference voltage measurement required to convert accelerations in g units. Since both transducers and accelerations were sampled successively, the total sample rate is 487Hz.

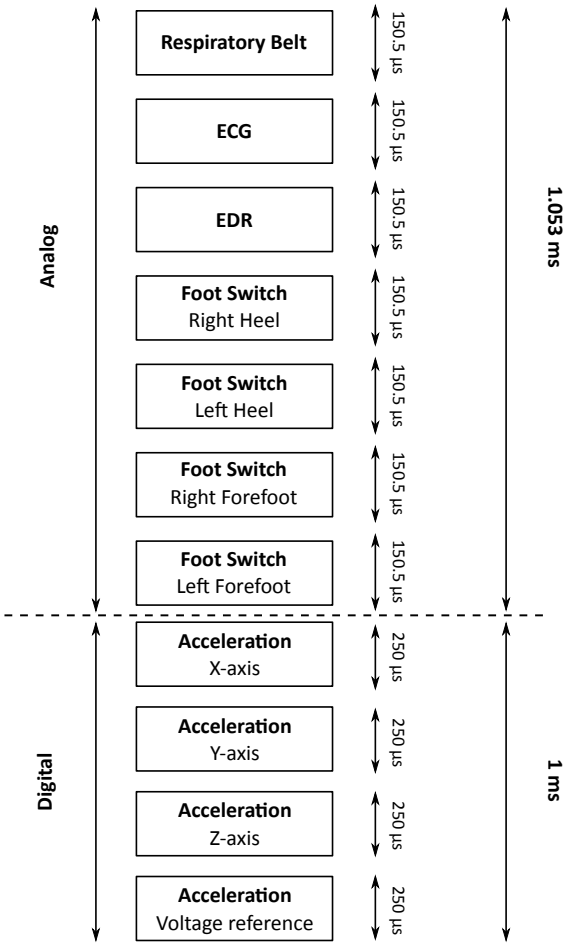

Figure 2: An overview of the sampling process.

The Hitachi H48C three-axis accelerometer is designed with an anti-aliasing filter, and is connected to a Microchip MCP 3204 12-bit ADC. Samples are retrieved through SPI, a serial protocol, at a rate of 1 kHz. The signal is oversampled to ensure that this filter is past the stopband and as such provides an improved noise floor. Force sensitive resistors (FSRs), produced by Interlinx FSR406, are used to measure gait temporal characteristics. The FSRs are placed on the heel and forefoot of the participant. The output of the FSR forms a voltage divider with a $1k\Omega$ resistor, whose output connects to a second order anti-aliasing low-pass filter that attenuates frequencies above 232.15 Hz.

The Electrodermal Response (EDR) is measured across two electrodes placed on the index and ring finger. The EDR signal is filtered through a band pass filter with a passband between 0.5 - 1.5Hz [30, 31]. The filter helps remove the shifting DC offset and higher frequency noise [30, 31]. The reference ground used for the non-measuring electrode has a current limit of 100nA, in an attempt to reduce the risk of electrical shock. The conditioned EDR signal is filtered by a second order, anti-aliasing low-pass filter that attenuates frequencies above 61.17 Hz.

A piezoelectric respiratory belt, produced by ADInstruments MLT1132, measures the respiration rate during ambulation through the volumetric change of the thoracic cavity. The respiratory signal is bandpass filtered by a voltage mode amplifier whose filter is designed with a passband between 0.13 - 0.5 Hz [32, 33]. The conditioned respiratory signal is filtered using an anti-aliasing filter that reduces frequencies above 1 Hz.

A three-lead ECG connected to the patient is measured during ambulation through the use of an instrumentation amplifier with a high common mode rejection ratio. An instrumentation amplifier is required to amplify the microvolt ECG signal. The output of the instrumentation amplifier is cascaded into a filter with a passband between 1 - 150 Hz to eliminate potential ADC saturation caused by a floating baseline and higher frequency noise. Lastly, an anti-aliasing filter reduces frequencies above 232.15 Hz.

The conditioned sensor output is connected to the ADC pins on the PIC24F that transmits the converted data to the Android Phone. The Processing Unit is powered via a 2000mAh lithium polymer (LiPo) battery, which is capable of an output voltage between 2.5V and 3.7V. The LiPo voltage is regulated to 5V, -5V and 3.3V in order to properly bias the biosensors, the conditioning circuitry and PIC24F. The current draw of the processing unit is approximately 900mA allowing for a continuous run time of 1 hour and 30 minutes, which is sufficient for the data collection in this paper, but may be too short for more extensive protocols. In the next section we describe the MCU software design to distinguish each sensor input and communicate them to Android device.

2.2. MCU Software Design

The embedded software was designed to continuously sample the conditioned biosignals through a 10-bit analog-to-digital converters (ADC) integrated with the PIC24F and through SPI when accelerations were measured. As outlined by the software architecture in Figure 3, the embedded software consists of several states.

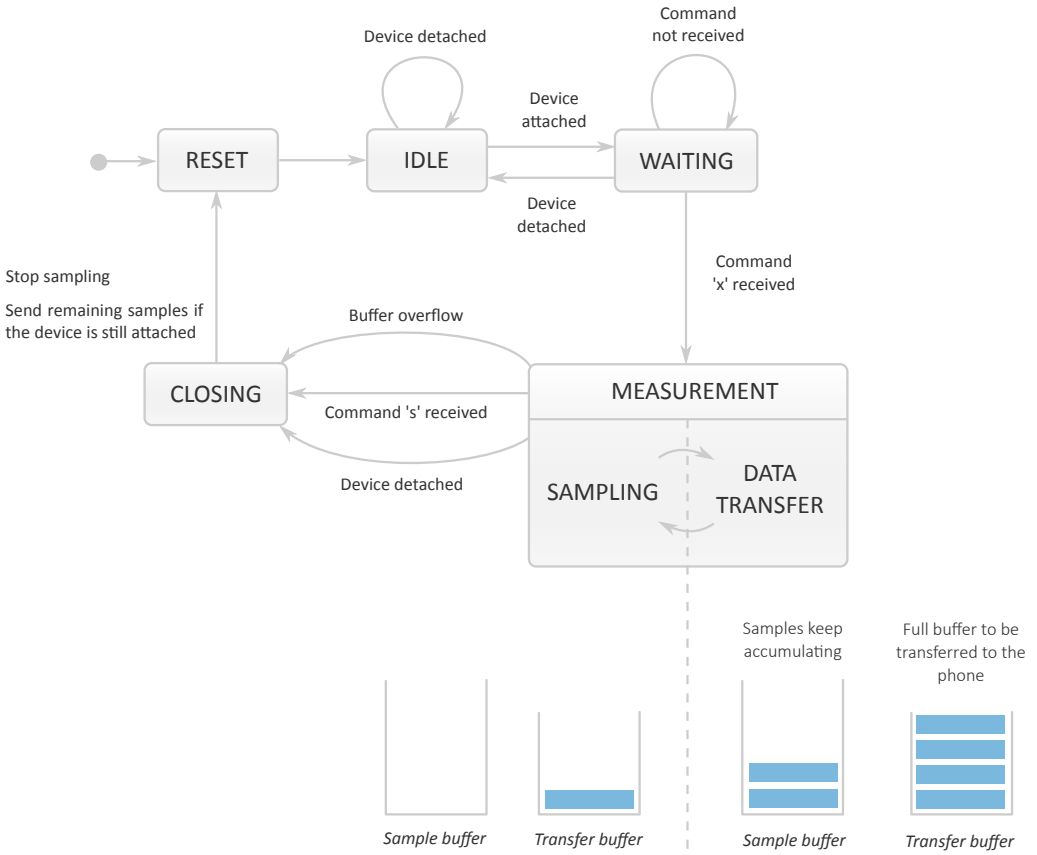

Figure 3: State machine on which was based our MCU software design.

The first state taken by the machine is the `RESET` state, in which timers, the 10-bit ADC and the modules required to communicate with the accelerometer are reset. Next, the machine enters immediately the `IDLE` state. In this one, the program waits for the smartphone to be connected to the processing unit. Once the former is attached, the machine enters the `WAITING` state, during which the processing unit waits for the phone to send a command. The latter consists of a single character `x`. If the phablet is detached, the program goes back to the `IDLE` state. Otherwise, the program enters the `MEASUREMENT` pseudo-state, composed of a `SAMPLING` state in which the wearable device samples data, and a `DATA TRANSFER` state, where data is transferred to the smartphone.

In the `SAMPLING` state, the device samples data and stores it in a transfer buffer that is later sent to the Android phone. The microcontroller alternates between the analog transducers and the accelerations sampling. Two interrupt service routines (ISR) are triggered in each case. ISRs are executed when special events are detected by the microcontroller. For our processing unit,

the first routine is executed when all of the analog transducers have been sampled. Every sample is associated to a channel so as to identify the origin of the measurement, and is placed into the transfer buffer mentioned earlier. The second ISR is designed to generate the signals required to retrieve data from the accelerometer. The data received from the SPI of the accelerometer is stored in the transfer buffer as well.

An arbitrary design choice was to limit the number of samples the transfer buffer can hold to 32 samples. Once this buffer is full, the program switches to the `DATA TRANSFER` state, during which the collected samples are transmitted to the smartphone as it provides a larger data storage capacity. A Microchip supplied Android USB Accessory Stack was used to allow the PIC24F to do so. ISRs can still be triggered during the `DATA TRANSFER` state. As a result, the data sampling does not stop even if the microcontroller is considered to be in a transfer state. Since the transfer buffer is full, another sample buffer, that is able to contain up to 1024 samples, stores measurements in the meantime. Before switching back to the `SAMPLING` state, the content of the sample buffer is moved to the the transfer buffer until the latter becomes full again.

The program alternates between the `SAMPLING` and the `DATA TRANSFER` states until either the phone sends a command (a single character `s`) that stops the sampling process, the phone is disconnected from the processing unit, or an overflow of the large sample buffer occurs. In that case, the program enters the `CLOSING` state: data sampling is stopped, and samples remaining in the buffers are transmitted to the phone if it is still attached. The program then enters the `RESET` state again.

2.3. Android Smartphone Datalogging

As it can be seen in Figure 4, a field in an Android application allows one to specify the amount of time during which the device attached to the smartphone should perform measurements. Data sampling will stop automatically after the specified duration. Below, the list of connected USB devices is displayed, although Figure 4 only shows an empty list since no devices were connected when the screenshot was taken. Finally, pressing the button under the list starts or stops data sampling.

The application uses the Accessory mode so as to exchange data with the processing unit. The Android operating system (OS) provides abstraction layers which allow one to receive data sent by the processing unit, by merely reading a file. In order to keep the user interface responsive, the

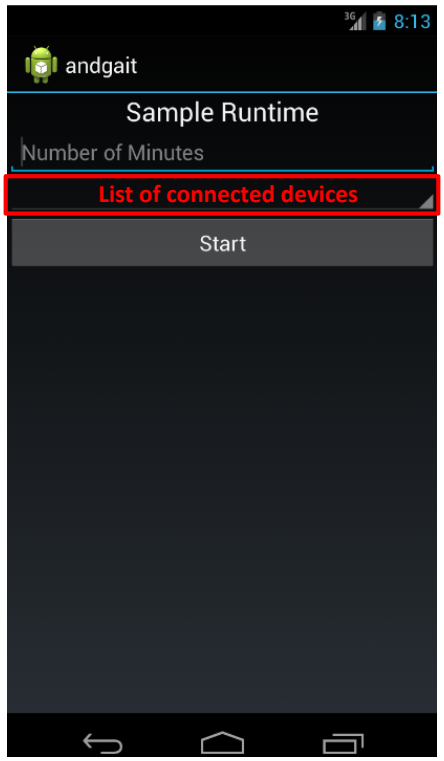

Figure 4: Screenshot of the Android application.

Android application creates a background service that polls the phone's USB receive buffers and stores the sampled data onto the phone's internal storage. The application keeps track of the service status, and updates the user interface accordingly. To avoid buffer overruns on the Smartphone CPU, the custom Android Application requests a CPU Wake Lock for the Android OS. A CPU Wake Lock prevents the Android OS from entering a low-power state.

3. Sampling methodology

The study was approved by the University of Pittsburgh's Institutional Review Board. Data was collected from 15 healthy participants (6 females, 9 males; 1.76 ± 0.11 m; 68.3 ± 9.68 kg; 20.2 ± 1.90 years; BMI: 22.1 ± 2.23). The participants were screened prior to testing for neurological and physiological conditions that would affect their gait. The anthropometric measures of height, weight, age and gender were obtained from the participant's prior to the experiment. After consenting to the study, participants were fitted with the device around the lumbar region, in order to position the accelerometer near the center-of-mass as suggested in previous studies (e.g., [34], [35]). Following

the sensor fitting step, participants performed two, fifteen-minute walking sessions around a closed corridor with a ten-minute break in-between. The placement of the Processing Unit was chosen to facilitate the collection of accelerometer signals for the exploration of non-linear stability analysis. During each session, the participant was instructed to focus strictly on the ambulation through the closed corridor. An investigator followed the participant and recorded any external stimuli that may have affected the gait. The investigator maintained a safe distance, approximately 35 feet, behind the participant so as not to modulate the participant's stride interval with the sound of periodic footfall [36]. No other external pacers were used in the study, but also no sources of pacing were noticed during walking. Participants were asked to wear comfortable footwear (e.g., running shoes). Sensor placements used in this study is shown in Figure 5.

4. Data analysis

4.1. Pre-Processing of signals

Although analog signal conditioning had greatly narrowed the frequency characteristics of the signals, various disturbances and noise were still present within the signals. To alleviate these issues, the collected data was pre-processed prior to further analysis. Some signals, such as the force sensitive resistors, required pre-processing in order to obtain relevant time series.

Stride interval time series: The purpose of the FSRs is to provide information concerning the stride interval time series from the heel impact and toe impact on each foot. We used a stride interval extraction algorithm proposed in [37], which is based on initially identifying potential strides, and then using probabilistic modeling and post-extraction filtering to determine stride interval time series from force sensitive resistor data. Stride intervals that were physiologically long or short (i.e., falling outside 0.01% and 99.99% of a gamma distribution fit) were removed. Ultimately, the average number of stride intervals across all participants per session was equal to 783 strides.

Heart rate variability (HRV): During the participant sessions, the ECG signal often exhibited motion artifacts [38] [39]. To alleviate the presence of these artifacts, a 15th-order low-pass Butterworth filter with the cut-off frequency equal to 40 Hz followed by a 23rd-order high-pass Butterworth filter with cutoff frequency equal to 1 Hz [40] was implemented. To extract the heart rate variability (HRV), we utilized a wavelet based algorithm to extract R peaks from ECG recordings

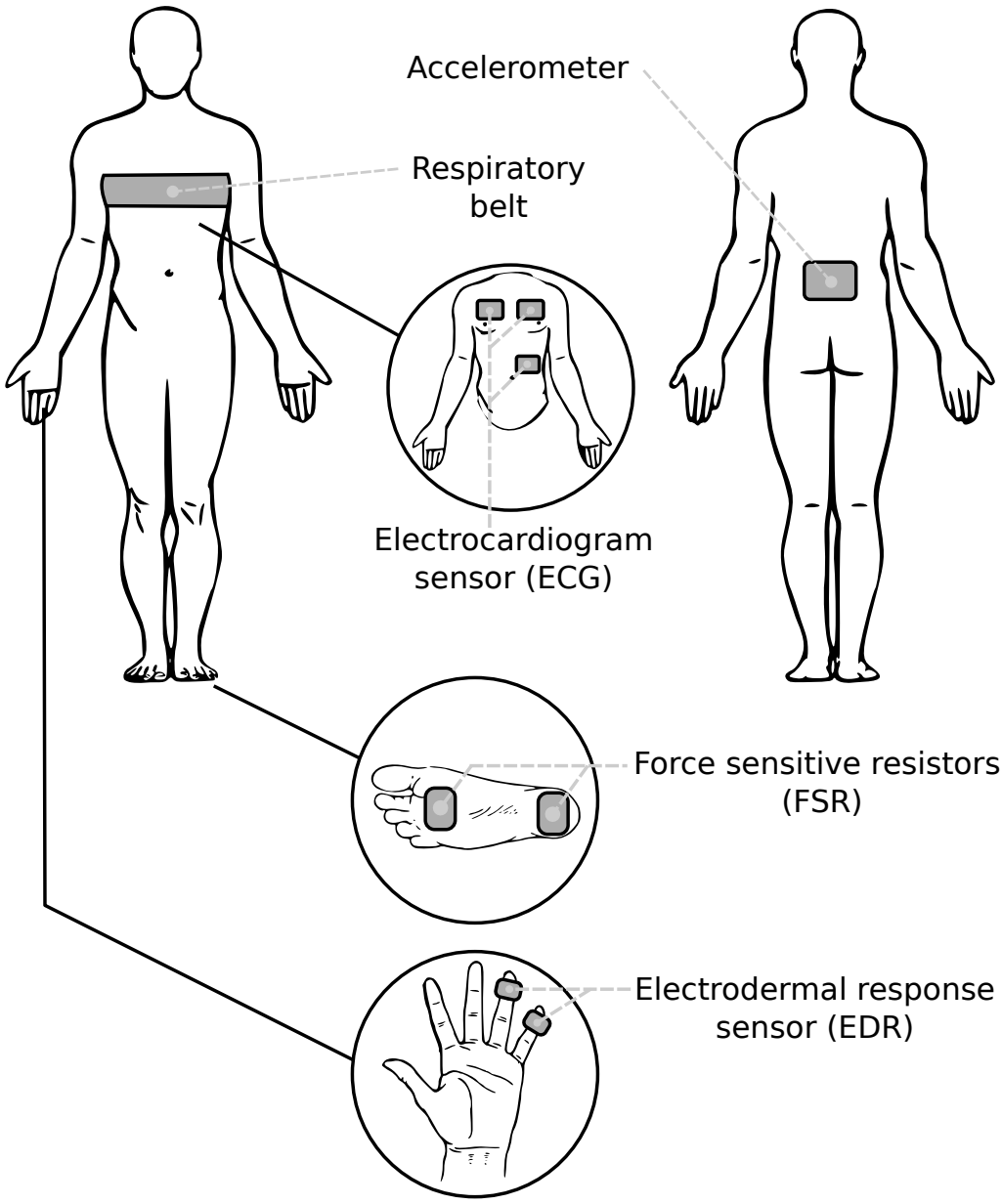

Figure 5: Sensor placements for all participants.

[41]. We subsequently eliminated points that fell outside 5% and 95% of a gamma distribution fit, considering these peaks as physiologically not relevant.

Respiratory rate (RR): To recover the respiratory rate from conditioned signals acquired,

we first utilized an 18th-order low-pass Butterworth filter with the cut-off frequency equal to 1.5 Hz [42]. Using the filtered signal, we found subsequent local maximal points under the following constraints: (a) successive points should be at least separated by 1 second; and (b) the detected maximal points should be greater than half of the standard deviation value of the filtered signal. These two constraints eliminate the detection of physiologically irrelevant points.

Electrodermal reactivity (EDR): To isolate the phasic response of the electrodermal reactivity signals, we utilized an 86th-order low-pass Butterworth filter with the cut-off frequency equal to 1.51 Hz followed by a 6th-order high-pass Butterworth filter with the cut-off frequency equal to 0.02 Hz [43], [44].

4.2. Feature extraction

The main purpose of the proposed system is to infer about various physiological systems during walking and the interactions amongst these systems. In order to do so, the proposed system should be able to extract certain features from each considered physiological system, and relate them to other features to infer about the walking condition of each person. As a preliminary step, we processed these signals offline, and in here, we extract features considered in previous contributions dealing with each of the considered physiological systems (e.g., [45], [46], [47], [48], [49], [50], [51], [52]). Not all features are not considered for all acquired signals, and presented results will make evident the considered features for each type of signals.

Assuming that a signal, $x(n)$, is represented by a set of N values, then using those values typical statistical features such as mean (μ_x), standard deviation (σ_x), the coefficient of variation (ξ_x), kurtosis (γ_x) can be calculated [53]. To assess the similarity between time structures of two signals, $x(n)$ and $y(n)$, we utilized the cross-correlation coefficient, CC_{x-y}, at the zeroth lag [53]. Variants of these statistical measures were further adopted to heart rate variability time series. Here, we considered SDNN, RMSSD, NN50, PNN50 which are typical statistical features used in the analysis of the HRV time series. For a thorough description of these variables, one should refer to [45], [46]. Here, we will only provide brief definitions of them. If we consider NN intervals (the so-called normal-to-normal intervals, that is, intervals between adjacent QRS complexes), then SDNN is defined as the standard deviation of NN intervals [45]. RMSSD is the square root of the mean squared differences of successive NN intervals [45]. NN50 is defined as the number of successive NN intervals greater than 50 ms [45]. PNN50 equals the number of NN50 divided by the total number

of NN intervals [45].

Stride interval dynamics incorporate temporal information into the analysis of the stride interval time series and reveals statistical persistence. Here, we utilized the spectral exponent, β, to characterize the stride interval dynamics as described in [49]. $\beta = 0$ indicates random, uncorrelated behavior (e.g. white Gaussian noise). $\beta = 1$ denotes a $1/f$ process, while $\beta = 2$ indicates a Brownian process [54]. It should be pointed that spectral exponent was also applied to heart rate time series [55] and respiratory rate time series [56].

In this paper, we also considered various information-theoretic features [47], [48], [50]. The Lempel-Ziv complexity (LZC) measures the predictability of the signal [50], [57]. The entropy rate (ρ) measure quantifies the extent of regularity in a signal [48]. A variant of the entropy rate known as the sample entropy (SampEn) is often used in the analysis of HRV time series [51], [52]. Extending the entropy rate measure, the cross-entropy rate, $\Lambda_{X|Y}$, quantifies the entropy rate between two stochastic processes [47]. This measure describes the predictability of a data point in one signal given a sequence of current and past data points in the other signal.

When considering features in the frequency domain, we considered the following three features [58]: the peak frequency, f_p, the spectral centroid, $\widehat{f}$, and the bandwidth, BW. Variants of these features known as very low frequency (VLF), low frequency (LF) and high frequency (HF) were also applied to the HRV time series [45].

Lastly, we considered a typically used time-frequency feature such as the wavelet entropy, Ω, for the analysis of acquired biomedical signals [59], [60].

4.3. Statistics

We used paired samples t-tests to examine whether there are any systematic differences between sessions in gait, skin conductance, respiration and heart rate measures; and used intraclass correlation coefficients (ICC) to quantify test-retest reliability between sessions. Next, we fit a series of multivariable linear mixed models using data from both sessions, with each measure as the dependent variable; sex, age, height and weight (simultaneously) as independent variables of interest; and a participant random effect to account for the correlation between sessions in the measurements from the same participant. We repeated modeling with BMI instead of height and weight. Associations were quantified as fixed effect regression coefficients corresponding to gender differences, and rates per unit for age (years), height (cm), weight (kg) and BMI (kg/m2). To

account for the large number of features considered, and the resulting number of hypothesis tests, we used false discovery rate methodology [61] to make multiplicity corrections to our p-values. Finally, using means across sessions, we computed Pearson correlation coefficients between gait features and other measures of skin conductance, respiration and heart rate. We used SAS version 9.2 (SAS Institute, Inc., Cary North Carolina) for all statistical analyses.

5. Results

Tables 1-6 summarize the average results of the feature extraction process for all 15 participants across the two sessions. The gait features considered in this manuscript are shown in Tables 1, 2 and 3, while Tables 4, 5, and 6 depict features associated with respiration, heart rate and electrodermal acitivity, respectively. Subscripts ML, AP and SI denote three anatomical directions: medio-lateral, anterior-posterior and superior-inferior, respectively. These are typical features considered in the literature for the given signals. The stride intervals did not differ based on the position (heel or toe) or leg (left or right) ($p > 0.11$). Hence, we considered stride interval time series from the left heel.

Table 1: Features based on stride intervals.

Feature	Session 1	Session 2	ICC
μ_s	1.18 ± 0.14	1.16 ± 0.16	0.90
ξ_s	6.07 ± 7.81	5.22 ± 7.66	0.49
β_s	0.33 ± 0.21	0.22 ± 0.28	0.17

There were no statistical differences in feature values between sessions ($p > 0.53$). No variables were dependent on age ($p > 0.14$), sex ($p > 0.71$), height ($p > 0.41$), weight ($p > 0.19$) and BMI ($p > 0.14$).

Among the considered features, a significant number of relations was determined between gait features and features based on other physiological signals. CC_{ML-AP} was negatively correlated with $f_{p_{EDR}}$ ($p = 0.03$), while $\Lambda_{ML|AP}$ and $\Lambda_{ML|SI}$ were positively correlated with the same variable ($p \leq 0.04$). BW_{ML} was positively correlated with LZC_{EDR} and $\widehat{f}_{EDR}$ ($p < 0.04$).

When considering the features based on the respiratory rate, we found that μ_{RR} was positively related to CC_{SI-AP}, $\Lambda_{ML|SI}$, $\widehat{f}_{ML}$, BW_{AP} and BW_{ML} ($p < 0.05$) and negatively related to ρ_{ML},

Table 2: Statistical and information-theoretic features based on gait accelerometry signals.

Feature	Session 1	Session 2	ICC
CC_{ML-AP}	0.10 ± 0.14	0.08 ± 0.12	0.98
CC_{ML-SI}	0.18 ± 0.12	0.20 ± 0.10	0.88
CC_{SI-AP}	0.06 ± 0.21	0.04 ± 0.16	0.95
LZC_{ML}	0.49 ± 0.03	0.48 ± 0.02	0.90
LZC_{AP}	0.46 ± 0.04	0.46 ± 0.04	0.93
LZC_{SI}	0.49 ± 0.02	0.49 ± 0.02	0.48
ρ_{ML}	0.77 ± 0.03	0.77 ± 0.02	0.87
ρ_{AP}	0.80 ± 0.03	0.80 ± 0.03	0.93
ρ_{SI}	0.78 ± 0.03	0.77 ± 0.02	0.57
$\Lambda_{ML\|AP}$	0.72 ± 0.07	0.71 ± 0.07	0.92
$\Lambda_{ML\|SI}$	0.69 ± 0.07	0.68 ± 0.08	0.92
$\Lambda_{AP\|SI}$	0.71 ± 0.09	0.71 ± 0.09	0.97

Table 3: Frequency and time-frequency features based on gait accelerometry signals.

Feature	Session 1	Session 2	ICC
$f_{p_{ML}}$	1.96 ± 1.16	2.91 ± 1.64	0.24
$\widehat{f}_{ML}$	5.67 ± 0.90	5.61 ± 0.84	0.96
BW_{ML}	4.80 ± 0.52	4.79 ± 1.45	0.97
$f_{p_{AP}}$	1.63 ± 0.11	1.65 ± 0.11	0.98
$\widehat{f}_{AP}$	4.17 ± 0.90	4.18 ± 0.91	0.97
BW_{AP}	4.20 ± 0.65	4.16 ± 0.58	0.82
$f_{p_{SI}}$	1.32 ± 0.69	1.87 ± 0.85	0.05
$\widehat{f}_{SI}$	4.81 ± 0.53	4.27 ± 0.50	0.88
BW_{SI}	4.71 ± 1.17	4.80 ± 1.07	0.82
Ω_{ML}	2.02 ± 0.21	1.95 ± 0.18	0.69
Ω_{AP}	0.38 ± 0.13	0.41 ± 0.13	0.85
Ω_{SI}	1.80 ± 0.54	1.87 ± 0.46	0.87

Table 4: Features based on EDR signals. * = multiplication by 1e-2

Feature	Session 1	Session 2	ICC
σ_{EDR}	0.15 ± 0.12	0.14 ± 0.09	0.63
γ_{EDR}	5.24 ± 3.37	4.01 ± 0.91	0.00
LZC_{EDR}	0.18 ± 0.03	0.19 ± 0.04	0.68
ρ_{EDR}*	93.6 ± 0.34	93.7 ± 0.35	0.56
$f_{p_{EDR}}$	0.07 ± 0.01	0.07 ± 0.02	0.00
$\widehat{f}_{EDR}$	0.26 ± 0.13	0.25 ± 0.15	0.69
BW_{EDR}	0.30 ± 0.11	0.32 ± 0.14	0.71

ρ_{AP} and $\widehat{f}_{SI}$ ($p \leq 0.04$). ξ_{RR} was increasing with the increasing values of the frequencies with the maximum spectral power in the SI direction ($p < 0.01$). A higher number of breaths per minute denoted higher regularity of ML and SI (ρ_{ML} and ρ_{AP}, $p \leq 0.01$) and higher values of $\widehat{f}_{ML}$ ($p = 0.03$), but also meant lower values of CC_{SI-AP}, LZC_{AP}, and BW_{ML} ($p \leq 0.04$). Lastly, higher β_{RR} meant a higher and wider spectral content of ML signals ($\widehat{f}_{ML}$ and BW_{ML}, $p < 0.04$), but also denoted smaller values of CC_{ML-AP}, $f_{p_{AP}}$, and Ω_{AP} ($p < 0.05$).

Table 5: Features based on respiratory rate time series. BRPM = breaths per minute.

Feature	Session 1	Session 2	ICC
μ_{RR}	3.49 ± 1.49	3.40 ± 1.21	0.94
ξ_{RR}	61.3 ± 10.2	62.5 ± 9.65	0.64
$BRPM$	19.1 ± 5.08	19.2 ± 4.82	0.93
β_{RR}	0.15 ± 0.28	0.16 ± 0.17	0.24

It should be also mentioned that a more peaked distribution of EDR amplitudes around the mean value (γ_{EDR}) also denoted higher sample entropies of HRV signals and a decreased spectral exponent (β_{RR}) of RR time series ($p < 0.04$).

Table 6: Features based on HRV time series. BPM = beats per minute.

Feature	Session 1	Session 2	ICC
μ_{HRV}	0.86 ± 0.25	0.89 ± 0.26	0.78
SDNN	0.17 ± 0.14	0.23 ± 0.21	0.93
ξ_{HRV}	17.0 ± 11.7	21.8 ± 15.0	0.91
BPM	75.0 ± 19.9	72.6 ± 18.8	0.75
RMSSD	0.22 ± 0.21	0.29 ± 0.27	0.92
NN50	193 ± 151	239 ± 186	0.81
PNN50	0.22 ± 0.19	0.26 ± 0.19	0.83
β_{HRV}	0.59 ± 0.16	0.66 ± 0.25	0.00
SamEn	1.50 ± 0.33	1.43 ± 0.36	0.48
VLF	0.49 ± 0.33	0.47 ± 0.33	0.45
LF	0.28 ± 0.18	0.28 ± 0.18	0.81
HF	0.18 ± 0.16	0.20 ± 0.17	0.23

6. Discussion

6.1. Multisystem interaction during walking

Many previous studies conjectured about the interactions between various physiological systems and human gait (e.g., [21], [62], [63]). However, those studies mostly correlated gait features obtained walking to features obtained from other physiological systems during sitting or standing. Our main contribution here is the system that can capture the interactions among different physiological systems, while the human body is in motion. Our results clearly demonstrated that in order to gain a clear understanding of human walking, cardiovascular system and autonomic control systems should be also monitored during walking. There was a clear interaction among these systems during simple walking tasks. We anticipate that walking trials involving challenges and/or multitasking will involve even greater interactions between these systems, as challenging walking trials and/or multitasking have effects on gait parameters [64], [65].

Previous contributions have shown that changes in the electrodermal activity can be detected during walking trials during which participants experience high anxiety regarding the possibility of falling [66], [67], [68]. However, our results have shown that the features based on electrodermal

activity were strongly related to gait features even during non-challenging walks. In fact, most of the EDR features were associated with one or more gait feature. The major implication of our findings is that the proposed device could be used to study locomotion and electrodermal coupling. This is especially significant in older adults with fear of falling as we can study the anxiety in older adults associated with increased postural threats [67].

While it is a known fact that breathing and walking are synchronized in humans [7], [69], we also found that several features of respiratory and locomotion systems are related as well. In particular, a breathing rate was strongly related to the spectral content and the variability of gait accelerometry signals, which is expected as the breathing rate is generally modulated by the pace of walking. The major implication of these results is the fact that the proposed device could be used to study locomotor-respiratory coupling during walking, as such studies are limited due to the lack of adequate systems. Most prior studies focused on the locomotor-respiratory coupling in balance studies. Nevertheless, the locomotor-respiratory coupling is important as energy-efficient and stable locomotion demands that the movement mechanical and metabolic demands are continuously met [70]. More specifically, the locomotion system generates motions and maintains stability, while the respiratory system maintains sufficient levels of oxygen while removing metabolic byproducts from the circulatory system [70]. However, it should be understood that these systems do not act independently. The locomotor system regulates the respiratory system by generating chemical and neural commands, while the respiratory system helps with the posture control as it continuously perturbed.

Similarly, HRV features were also related to gait accelerometry features and the major implication of our work is that the proposed device can used to study cardiolocomotor coupling. As in the case of features based on the respiratory rate time series, the HRV features directly inferred about the spectral characteristics and the variability of gait accelerometry signals. Our findings support the previous contributions which showed that the cardiac rhythm is controlled by the locomotor system (i.e., the locomotor system's rhythm) [71]. The cardiolocomotor interaction can possibly indicate direct interactions between the cardiovascular centers and the central pattern generator [71], which can lead to many interesting investigations using the proposed devices such as investigations of the cardiolocomotor coupling in patients with compromised cardiovascular systems due to myocardial infraction or other similar cardiovascular diseases.

The test-retest reliability of the considered features is good or excellent for 42 out of 50 features, while only 8 out of 50 features had poor reliability ($ICC < 0.4$). These findings point out that the proposed system is capable of measuring the considered physiological signals reliably. Specifically, low ICC values are spread across different physiological signals, and other features considered for those signals had good or excellent ICC values. It was interesting to note that the spectral exponent feature had low ICC values in all considered cases. In addition, other four frequency features ($f_{p_{ML}}$, $f_{p_{SI}}$, $f_{p_{EDR}}$ and HF) also had very low ICC values. While there is no obvious reason why these frequency-based features should have low ICC values, future investigations should consider them more closely.

6.2. Remarks

The proposed system is a prototype system developed to demonstrate that multisystem interactions should be considering during walking. Our future work involves two directions. One direction is the development of sensors that will connect to the central processing unit, shown in Figure 1, via a wireless protocol (e.g., Bluetooth). This will enables us to avoid any cables currently needed to connect sensors, and decrease any complications while using a system (e.g., long set-up times or additional walking hazards due to long cables). Our second direction will be focused towards the implementation of some of the signal processing algorithms on the smart phone, which would enable processing of data in real time. Real time data processing is desirable for future versions of this device, so that the proposed device is enabled to detect walking instabilities in real time in order to prevent falls. A real time analysis of walking instabilities can increase research and clinical potentials of the proposed device. However, it should be pointed out that selected features will be implemented and those features will be selected based on our future studies with a clinical population. A possible solution for data processing is that the phone uploads collected points to a cloud based unit, which will process signal samples as they arrive. In such a scenario, it would be worthwhile to compress data on the smartphone in order to reduce the burden on wireless networks and the subscriber wireless data plan. Lastly, we need to investigate the power efficiency of the device in order to enable the device for longer data collections.

Additionally, the presented results are the first step towards the investigations of multisystem physiological interactions. While most of our efforts in the present manuscript are geared towards the establishing the reliability of the results with the proposed system, our future investigations will

be aimed towards examining walking under different conditions, but also investigations of specific interactions and the effects of various neuro-degenerative diseases on these interactions. Finally, our findings were based on a relatively small sample of participants. Further study is needed to validate our findings and draw more definitive conclusions.

Future developments should also consider how to utilize the proposed device for assessing sit-to-stand maneuvers. Sit-to-stand performance is also affected by many physiological variables [72].

7. Conclusion

In this paper, we proposed a smart-phone based gait monitor capable of simultaneously acquiring data from multiple physiological systems involved in human walking. For the purpose of this study, we collected data from 15 healthy subjects during 15-minute overground walks at a self-selected speed. The data was collected using the proposed system and stored for offline analyses. Our numerical analysis involved feature extraction in time, frequency and time-frequency domains. The results of our analysis clearly showed that multisystem interaction existed during walking.

Acknowledgments

This work was supported in part by the Pittsburgh Claude D. Pepper Older Americans Independence Center (NIA P30 AG 024827).

References

[1] J. M. Guralnik, L. Ferrucci, C. F. Pieper, S. G. Leveille, K. S. Markides, G. V. Ostir, S. Studenski, L. F. Berkman, and R. B. Wallace, "Lower extremity function and subsequent disability," *The Journals of Gerontology Series A: Biological Sciences and Medical Sciences*, vol. 55, no. 4, pp. M221–M231, Apr. 2000.

[2] M. Cesari, S. B. Kritchevsky, B. W. H. J. Penninx, B. J. Nicklas, E. M. Simonsick, A. B. Newman, F. A. Tylavsky, J. S. Brach, S. Satterfield, D. C. Bauer, M. Visser, S. M. Rubin, T. B. Harris, and M. Pahor, "Prognostic value of usual gait speed in well-functioning older peopleresults from the health, aging and body composition study," *Journal of the American Geriatrics Society*, vol. 53, no. 10, pp. 1675–1680, Oct. 2005.

[3] T. K. DeMott, J. K. Richardson, S. B. Thies, and J. A. Ashton-Miller, "Falls and gait characteristics among older persons with peripheral neuropathy," *American Journal of Physical Medicine and Rehabilitation*, vol. 86, no. 2, pp. 125–132, Feb. 2007.

[4] A. C. Scheffer, M. J. Schuurmans, N. van Dijk, T. van der Hooft, and S. E. de Rooij, "Fear of falling: measurement strategy, prevalence, risk factors and consequences among older persons," *Age and Ageing*, vol. 37, no. 1, pp. 19–24, Jan. 2008.

[5] R. Boyd and J. Stevens, "Falls and fear of falling: burden, beliefs and behaviours," *Age and Ageing*, vol. 38, no. 4, pp. 423–428, 2009.

[6] M. F. Reelick, M. B. van Iersel, R. P. C. Kessels, and M. G. M. Olde Rikkert, "The influence of fear of falling on gait and balance in older people," *Age and Ageing*, vol. 38, no. 4, pp. 435–440, 2009.

[7] J. E. Clague, P. J. Petrie, and M. A. Horan, "Hypocapnia and its relation to fear of falling," *Archives of Physical Medicine and Rehabilitation*, vol. 81, no. 11, pp. 1485–1488, Nov. 2000.

[8] S. D. Kreibig, F. H. Wilhelm, W. T. Roth, and J. J. Gross, "Cardiovascular, electrodermal, and respiratory response patterns to fear- and sadness-inducing films," *Psychophysiology*, vol. 44, no. 5, pp. 787–806, Sep. 2007.

[9] S. D. Kreibig, "Autonomic nervous system activity in emotion: A review," *Biological Psychology*, vol. 84, no. 3, pp. 394 – 421, Jul. 2010.

[10] V. Magagnin, A. Porta, L. Fusini, V. Licari, I. Bo, M. Turiel, F. Molteni, S. Cerutti, and E. G. Caiani, "Evaluation of the autonomic response in healthy subjects during treadmill training with assistance of a robot-driven gait orthosis," *Gait and Posture*, vol. 29, no. 3, pp. 504–508, Apr. 2009.

[11] J. S. Brach, R. Berthold, R. Craik, J. M. VanSwearingen, and A. B. Newman, "Gait variability in community-dwelling older adults," *Journal of the American Geriatrics Society*, vol. 49, no. 12, pp. 1646–1650, Dec. 2001.

[12] M. S. Orendurff, A. D. Segal, J. S. Berge, K. C. Flick, D. Spanier, and G. K. Klute, "The

kinematics and kinetics of turning: limb asymmetries associated with walking a circular path," *Gait and Posture*, vol. 23, no. 1, pp. 106–111, Jan. 2006.

[13] J. G. Richards, "The measurement of human motion: A comparison of commercially available systems," *Human Movement Science*, vol. 18, no. 5, pp. 589–602, Oct. 1999.

[14] S. Damouras, M. D. Chang, E. Sejdić, and T. Chau, "An empirical examination of detrended fluctuation analysis for gait data," *Gait and Posture*, vol. 31, no. 3, pp. 336–340, Mar. 2010.

[15] I. Schwartz, A. Sajin, I. Fisher, M. Neeb, M. Shochina, M. Katz-Leurer, and Z. Meiner, "The effectiveness of locomotor therapy using robotic-assisted gait training in subacute stroke patients: A randomized controlled trial," *PM&R*, vol. 1, no. 6, pp. 516 – 523, Jun. 2009.

[16] J. A. Blaya and H. Herr, "Adaptive control of a variable-impedance ankle-foot orthosis to assist drop-foot gait," *IEEE Transactions on Neural Systems and Rehabilitation Engineering*, vol. 12, no. 1, pp. 24–31, Mar. 2004.

[17] S. Bamberg, A. Y. Benbasat, D. M. Scarborough, D. E. Krebs, and J. A. Paradiso, "Gait analysis using a shoe-integrated wireless sensor system," *IEEE Transactions on Information Technology in Biomedicine*, vol. 12, no. 4, pp. 413–423, Jul. 2008.

[18] M. Chen, B. Huang, and Y. Xu, "Intelligent shoes for abnormal gait detection," in *Proc. of IEEE International Conference on Robotics and Automation (ICRA 2008)*, Pasadena, CA, USA, May 2008, pp. 2019–2024.

[19] K. Kong and M. Tomizuka, "A gait monitoring system based on air pressure sensors embedded in a shoe," *IEEE/ASME Transactions on Mechatronics*, vol. 14, no. 3, pp. 358–370, Jun. 2009.

[20] U. Anliker, J. A. Ward, P. Lukowicz, G. Troster, F. Dolveck, M. Baer, F. Keita, E. B. Schenker, F. Catarsi, L. Coluccini, A. Belardinelli, D. Shklarski, M. Alon, E. Hirt, R. Schmid, and M. Vuskovic, "AMON: a wearable multiparameter medical monitoring and alert system," *IEEE Transactions on Information Technology in Biomedicine*, vol. 8, no. 4, pp. 415–427, Dec. 2004.

[21] T. Vuorela, V.-P. Seppa, J. Vanhala, and J. Hyttinen, "Design and implementation of a

portable long-term physiological signal recorder," *IEEE Transactions on Information Technology in Biomedicine*, vol. 14, no. 3, pp. 718–725, May 2010.

[22] M. L. Fruin and J. W. Rankin, "Validity of a multi-sensor armband in estimating rest and exercise energy expenditure," *Medicine and Science in Sports and Exercise*, vol. 36, no. 6, pp. 1063–1069, Jun. 2004.

[23] P. Kugler, C. Jaremenko, J. Schlachetzki, J. Winkler, J. Klucken, and B. Eskofier, "Automatic recognition of parkinson's disease using surface electromyography during standardized gait tests," in *35th Annual International Conference of the IEEE Engineering in Medicine and Biology Society (EMBC 2013)*, Osaka, Japan, Jul. 2013, pp. 5781–5784.

[24] K. J. Heilman and S. W. Porges, "Accuracy of the LifeShirt (Vivometrics) in the detection of cardiac rhythms," *Biological Psychology*, vol. 75, no. 3, pp. 300–305, Jul. 2007.

[25] T. Linz, R. Vieroth, C. Dils, M. Koch, T. Braun, K. F. Becker, C. Kallmayer, and S. M. Hong, "Embroidered interconnections and encapsulation for electronics in textiles for wearable electronics applications," *Advances in Science and Technology*, vol. 60, pp. 85–94, 2008.

[26] N. Noury, A. Dittmar, C. Corroy, R. Baghai, J. L. Weber, D. Blanc, F. Klefstat, A. Blinovska, S. Vaysse, and B. Comet, "VTAMN - a smart clothe for ambulatory remote monitoring of physiological parameters and activity," in *Proc. of 26th Annual International Conference of the IEEE Engineering in Medicine and Biology Society (EMBS '04)*, San Francisco, CA, USA, Sep. 2004, pp. 3266–3269.

[27] R. Paradiso, G. Loriga, and N. Taccini, "A wearable health care system based on knitted integrated sensors," *IEEE Transactions on Information Technology in Biomedicine*, vol. 9, no. 3, pp. 337–344, Sep. 2005.

[28] S. Nishiguchi, M. Yamada, K. Nagai, S. Mori, Y. Kajiwara, T. Sonoda, K. Yoshimura, H. Yoshitomi, H. Ito, K. Okamoto, T. Ito, S. Muto, T. Ishihara, and T. Aoyama, "Reliability and validity of gait analysis by Android-based smartphone," *Telemedicine and e-Health*, vol. 18, no. 4, pp. 292–296, May 2012.

[29] J. Juen, Q. Cheng, V. Prieto-Centurion, J. A. Krishnan, and B. Schatz, "Health monitors

for chronic disease by gait analysis with mobile phones," *Telemedicine and e-Health*, vol. 20, no. 11, pp. 1035–1041, Nov. 2014.

[30] J. Schumm, M. Bachlin, C. Setz, B. Arnrich, D. Roggen, and G. Troster, "Effect of movements on the electrodermal response after a startle event," in *Proc. of Second International Conference on Pervasive Computing Technologies for Healthcare (PervasiveHealth 2008)*, Tampere, Finland, Jan.-Feb. 30-1, 2008, pp. 315–318.

[31] C. Setz, B. Arnrich, J. Schumm, R. La Marca, G. Troster, and U. Ehlert, "Discriminating stress from cognitive load using a wearable eda device," *IEEE Transactions on Information Technology in Biomedicine*, vol. 14, no. 2, pp. 410–417, Mar. 2010.

[32] J. H. Houtveen, P. F. C. Groot, and E. J. C. de Geus, "Validation of the thoracic impedance derived respiratory signal using multilevel analysis," *International Journal of Psychophysiology*, vol. 59, no. 2, pp. 97–106, 2006.

[33] J. M. Ernst, D. A. Litvack, D. L. Lozano, J. T. Cacioppo, and G. G. Berntson, "Impedance pneumography: Noise as signal in impedance cardiography," *Psychophysiology*, vol. 36, no. 3, pp. 333–338, May 1999.

[34] R. Moe-Nilssen and J. L. Helbostad, "Estimation of gait cycle characteristics by trunk accelerometry," *Journal of Biomechanics*, vol. 37, no. 1, pp. 121–126, Jan. 2004.

[35] M. Henriksen, H. Lund, R. Moe-Nilssen, H. Bliddal, and B. Danneskiod-Samsoe, "Test-retest reliability of trunk accelerometric gait analysis," *Gait and Posture*, vol. 19, no. 3, pp. 288–297, Jun. 2004.

[36] E. Sejdić, Y. Fu, A. Pak, J. A. Fairley, and T. Chau, "The effects of rhythmic sensory cues on the temporal dynamics of human gait," *PLoS ONE*, vol. 7, no. 8, pp. e43 104–1–7, Aug. 2012.

[37] T. Chau and S. Rizvi, "Automatic stride interval extraction from long, highly variable and noisy gait timing signals," *Human Movement Science*, vol. 21, no. 4, pp. 495–514, Oct. 2002.

[38] T. Pawar, N. S. Anantakrishnan, S. Chaudhuri, and S. P. Duttagupta, "Impact of ambulation in wearable-ECG," *Annals of Biomedical Engineering*, vol. 36, no. 9, pp. 1547–1557, Sep. 2008.

[39] ——, "Transition detection in body movement activities for wearable ECG," *IEEE Transactions on Biomedical Engineering*, vol. 54, no. 6, pp. 1149–1152, Jun. 2007.

[40] S. Luo and P. Johnston, "A review of electrocardiogram filtering," *Journal of Electrocardiology*, vol. 43, no. 6, pp. 486–496, Nov. - Dec. 2010.

[41] C. Li, C. Zheng, and C. Tai, "Detection of ECG characteristic points using wavelet transforms," *IEEE Transactions on Biomedical Engineering*, vol. 42, no. 1, pp. 21–28, Jan. 1995.

[42] K. Nakajima, T. Tamura, and H. Miike, "Monitoring of heart and respiratory rates by photoplethysmography using a digital filtering technique," *Medical Engineering and Physics*, vol. 18, no. 5, pp. 365–372, Jul. 1996.

[43] M.-Z. Poh, N. C. Swenson, and R. W. Picard, "A wearable sensor for unobtrusive, long-term assessment of electrodermal activity," *IEEE Transaction on Biomedical Engineering*, vol. 57, no. 5, pp. 1243–1252, May 2010.

[44] D. R. Bach, G. Flandin, K. J. Friston, and R. J. Dolan, "Modelling event-related skin conductance responses," *International Journal of Psychophysiology*, vol. 75, no. 3, pp. 349–356, Mar. 2010.

[45] Task Force of the European Society of Cardiology the North American Society of Pacing, "Heart rate variability: Standards of measurement, physiological interpretation, and clinical use," *Circulation*, vol. 93, no. 5, pp. 1043–1065, Mar. 1996.

[46] U. R. Acharya, K. P. Joseph, N. Kannathal, C. M. Lim, and J. S. Suri, "Heart rate variability: a review," *Medical and Biological Engineering and Computing*, vol. 44, no. 12, pp. 1031–1051, Dec. 2006.

[47] A. Porta, S. Guzzetti, N. Montano, M. Pagani, V. Somers, A. Malliani, G. Baselli, and S. Cerutti, "Information domain analysis of cardiovascular variability signals: Evaluation of regularity, synchronisation and co-ordination," *Medical and Biological Engineering and Computing*, vol. 38, no. 2, pp. 180–188, Mar. 2000.

[48] A. Porta, S. Guzzetti, N. Montano, R. Furlan, M. Pagani, A. Malliani, and S. Cerutti, "Entropy, entropy rate, and pattern classification as tools to typify complexity in short heart

period variability series," *IEEE Transactions on Biomedical Engineering*, vol. 48, no. 11, pp. 1282–1291, Nov. 2001.

[49] A. Schaefer, J. S. Brach, S. Perera, and E. Sejdić, "A comparative analysis of spectral exponent estimation techniques for $1/f^{\beta}$ processes with applications to the analysis of stride interval time series," *Journal of Neuroscience Methods*, vol. 222, pp. 118–130, Jan. 2014.

[50] M. Aboy, R. Hornero, D. Abasolo, and D. Alvarez, "Interpretation of the Lempel-Ziv complexity measure in the context of biomedical signal analysis," *IEEE Transactions on Biomedical Engineering*, vol. 53, no. 11, pp. 2282–2288, Nov. 2006.

[51] D. E. Lake, J. S. Richman, M. P. Griffin, and J. R. Moorman, "Sample entropy analysis of neonatal heart rate variability," *American Journal of Physiology - Regulatory, Integrative and Comparative Physiology*, vol. 283, no. 3, pp. R789–R797, Sep. 2002.

[52] H. M. Al-Angari and A. V. Sahakian, "Use of sample entropy approach to study heart rate variability in obstructive sleep apnea syndrome," *IEEE Transactions on Biomedical Engineering*, vol. 54, no. 10, pp. 1900–1904, Oct. 2007.

[53] A. Papoulis, *Probability, Random Variables, and Stochastic Processes*, 3rd ed. New York: WCB/McGraw-Hill, 1991.

[54] E. Sejdić and L. A. Lipsitz, "Necessity of noise in physiology and medicine," *Computer Methods and Programs in Biomedicine*, vol. 111, no. 2, pp. 459–470, Aug. 2013.

[55] A. Bunde, S. Havlin, J. W. Kantelhardt, T. Penzel, J.-H. Peter, and K. Voigt, "Correlated and uncorrelated regions in heart-rate fluctuations during sleep," *Physical Review Letters*, vol. 85, no. 17, pp. 3736–3739, Oct. 2000.

[56] D. N. Baldwin, B. Suki, J. J. Pillow, H. L. Roiha, S. Minocchieri, and U. Frey, "Effect of sighs on breathing memory and dynamics in healthy infants," *Journal of Applied Physiology*, vol. 97, no. 5, pp. 1830–1839, Nov. 2004.

[57] A. Lempel and J. Ziv, "On the complexity of finite sequences," *IEEE Transactions on Information Theory*, vol. 22, no. 1, pp. 75–81, Jan. 1976.

[58] E. Sejdić, C. M. Steele, and T. Chau, "The effects of head movement on dual-axis cervical accelerometry signals," *BMC Research Notes*, vol. 3, pp. 269–1–6, 2010.

[59] E. Sejdić, I. Djurović, and J. Jiang, "Time-frequency feature representation using energy concentration: An overview of recent advances," *Digital Signal Processing*, vol. 19, no. 1, pp. 153–183, Jan. 2009.

[60] E. Sejdić, K. A. Lowry, J. Bellanca, M. S. Redfern, and J. S. Brach, "A comprehensive assessment of gait accelerometry signals in time, frequency and time-frequency domains," *IEEE Transactions on Neural Systems and Rehabilitation Engineering*, vol. 22, no. 3, pp. 603–612, May 2014.

[61] Y. Benjamini and Y. Hochberg, "Controlling the false discovery rate: A practical and powerful approach to multiple testing," *Journal of the Royal Statistical Society. Series B (Methodological)*, vol. 57, no. 1, pp. 289–300, 1995.

[62] M.-C. Chiu and M.-J. Wang, "The effect of gait speed and gender on perceived exertion, muscle activity, joint motion of lower extremity, ground reaction force and heart rate during normal walking," *Gait and Posture*, vol. 25, no. 3, pp. 385–392, Mar. 2007.

[63] K. M. Sibley, G. Mochizuki, J. G. Esposito, J. M. Camilleri, and W. E. McIlroy, "Phasic electrodermal responses associated with whole-body instability: Presence and influence of expectation," *Brain Research*, vol. 1216, pp. 38–45, Jun. 2008.

[64] H. B. Menz, S. R. Lord, and R. C. Fitzpatrick, "Acceleration patterns of the head and pelvis when walking on level and irregular surfaces," *Gait and Posture*, vol. 18, no. 1, pp. 35–46, Aug. 2003.

[65] W. A. Sparrow, E. J. Bradshaw, E. Lamoureux, and O. Tirosh, "Ageing effects on the attention demands of walking," *Human Movement Science*, vol. 21, no. 5-6, pp. 961–972, Dec. 2002.

[66] A. L. Adkin, J. S. Frank, M. G. Carpenter, and G. W. Peysar, "Fear of falling modifies anticipatory postural control," *Experimental Brain Research*, vol. 143, no. 2, pp. 160–170, Mar. 2002.

[67] W. H. Gage, R. J. Sleik, M. A. Polych, N. C. McKenzie, and L. A. Brown, "The allocation of attention during locomotion is altered by anxiety," *Experimental Brain Research*, vol. 150, no. 3, pp. 385–394, Jun. 2003.

[68] L. A. Brown, R. J. Sleik, M. A. Polych, and W. H. Gage, "Is the prioritization of postural control altered in conditions of postural threat in younger and older adults?" *The Journals of Gerontology Series A: Biological Sciences and Medical Sciences*, vol. 57, no. 12, pp. M785–M792, Dec. 2002.

[69] S. Schiermeier, D. Schafer, T. Schafer, W. Greulich, and M. E. Schlafke, "Breathing and locomotion in patients with Parkinson's disease," *Pflugers Archiv - European Journal of Physiology*, vol. 443, no. 443, pp. 67–71, Oct. 2001.

[70] R. E. A. Van Emmerik, J. Hamill, and W. J. McDermott, "Variability and coordinative function in human gait," *Quest*, vol. 57, no. 1, pp. 102–123, 2005.

[71] K. Nomura, Y. Takei, and Y. Yanagida, "Comparison of cardio-locomotor synchronization during running and cycling," *European Journal of Applied Physiology*, vol. 89, no. 3/4, pp. 221–229, May 2003.

[72] S. R. Lord, S. M. Murray, K. Chapman, B. Munro, and A. Tiedemann, "Sit-to-stand performance depends on sensation, speed, balance, and psychological status in addition to strength in older people," *The Journals of Gerontology: Series A*, vol. 57, no. 8, pp. M539–M543, Aug. 2002.